

See discussions, stats, and author profiles for this publication at: <https://www.researchgate.net/publication/51189568>

# Modulated FT-Raman Fiber-Optic Spectroscopy: A Technique for Remotely Monitoring High- Temperature Reactions in Real-Time

ARTICLE *in* ANALYTICAL CHEMISTRY · JUNE 1997

Impact Factor: 5.64 · DOI: 10.1021/ac970193h · Source: PubMed

---

CITATIONS

17

---

READS

16

3 AUTHORS, INCLUDING:



John B. Cooper

Old Dominion University

44 PUBLICATIONS 780 CITATIONS

SEE PROFILE

## Accelerated Articles

# Modulated FT-Raman Fiber-Optic Spectroscopy: A Technique for Remotely Monitoring High-Temperature Reactions in Real-Time

John B. Cooper,<sup>\*,†</sup> Kent L. Wise,<sup>†</sup> and Brian J. Jensen<sup>‡</sup>

Department of Chemistry and Biochemistry, Old Dominion University, Norfolk, Virginia 23529, and NASA Langley Research Center, Hampton, Virginia 23681

**A modification to a commercial FT-Raman spectrometer is presented for the elimination of thermal backgrounds in FT-Raman spectra. The modification involves the use of a mechanical chopper to modulate the CW laser, remote collection of the signal via fiber optics, and connection of a dual-phase digital signal processor lock-in amplifier between the detector and the spectrometer's collection electronics to demodulate and filter the optical signals. The resulting modulated FT-Raman fiber-optic spectrometer is capable of completely eliminating thermal backgrounds at temperatures exceeding 370 °C. In addition, the signal/noise of generated Raman spectra is greater than for spectra collected with the conventional FT-Raman under identical conditions and incident laser power. This is true for both room-temperature and hot samples. The method allows collection of data using preexisting spectrometer software. The total cost of the modification (excluding fiber optics) is ~\$3000 and requires less than 2 h to implement. This is the first report of FT-Raman spectra collected at temperatures in excess of 300 °C in the absence of thermal backgrounds.**

Recent research in our group has focused on using fiber-optic Raman spectroscopy to monitor the high-temperature curing of high performance polymers for the aerospace industry.<sup>1,2</sup> One approach that has been successful is the use of a dispersive Raman instrument using short-wavelength near-IR radiation (~800 nm).<sup>2</sup> Although for many polymer cures this approach is feasible,

polymers that are highly fluorescent still present an obstacle. In particular, modified polyimides represent the largest and most promising class of high-temperature polymers<sup>3</sup> and yet cannot be analyzed with dispersive instruments due to their intense fluorescence. Due to longer wavelength excitation, FT-Raman instruments do allow the acquisition of polyimide Raman spectra at room temperature, but these spectra cannot be acquired within the autoclave in real-time due to the thermal background which occurs at the high temperatures required for processing. This ability for real-time in situ monitoring is crucial if intelligent feedback systems based on direct chemical information are to be designed for processing autoclaves.

Several researchers have addressed the problem of thermal backgrounds in FT-Raman spectra. Cutler et al. have successfully removed thermal backgrounds by synchronizing a Q-switched pulsed laser to the interferometer reference laser fringe crossings and adjusting the A/D sampling of the spectrometer so that it coincides with the peak of the detector pulses.<sup>4</sup> This approach has also been used in combination with a fast analog filter to improve signal/noise and to discriminate against long-lived backgrounds.<sup>5,6</sup> A second improvement is the use of a ratioing circuit to minimize pulse-to-pulse fluctuations of the Q-switched laser and thus further improve signal/noise.<sup>7</sup> Sakamoto and co-workers developed an asynchronous method to eliminate thermal backgrounds using a Q-switched pulsed laser in combination with a gate circuit and a low-pass filter which avoids the necessity of triggering the laser using the interferometer reference laser fringe

<sup>†</sup> Old Dominion University.

<sup>‡</sup> NASA Langley Research Center.

(1) Cooper, J. B.; Vess, T. M.; Wise, K. L.; Campbell, L.; Flecher, P.; Albin, S. *Recent Res. Dev. Opt. Eng.* **1996**, *1*, 23.

(2) Cooper, J. B.; Vess, T. M.; Campbell, L. A.; Jensen, B. J. *J. Appl. Polym. Sci.* **1996**, *62*, 135.

(3) Hou, T. H.; Jensen, B. J.; Hergenrother, P. M. *Compos. Mater.* **1996**, *30*, 109.

(4) Cutler, D. J.; Mould, H. M.; Bennett, B.; Turner, A. J. *J. Raman Spectrosc.* **1991**, *22*, 367.

(5) Petty, C. J.; Bennett, B. *Spectrochim. Acta* **1990**, *41*, 331.

(6) Cutler, D. J. *Spectrochim. Acta* **1990**, *41*, 131.

(7) Cutler, D. J.; Petty, C. J. *Spectrochim. Acta* **1991**, *47*, 1159.

crossings.<sup>8</sup> One drawback of all of these approaches is the use of slow mirror velocities, resulting in longer acquisition times for individual spectra relative to a conventional FT-Raman experiment. In addition, the short laser pulse widths (ranging from 7 to 100 ns) and thus high laser peak powers result in a greater probability of laser-induced sample degradation. Bennett also described an approach using a diode-pumped pulsed laser in combination with a sample and hold circuit which is triggered off of the A/D converter.<sup>9</sup> This approach can be performed either synchronously or asynchronously (with respect to the A/D sampling); however, either method requires specialty software to reconstruct the Raman spectrum. In addition, Bennett stated that optimum performance is achieved at slow interferometer mirror velocities (0.1 cm/s) which results in longer acquisition times. Recently, Petty described a method to eliminate thermal backgrounds using a modulated laser and a step-scan FT-Raman spectrometer.<sup>10</sup> Although successful, the step-scan experiment requires much longer single-spectrum acquisition times when compared to a conventional FT-Raman. When time-dependent reactions are monitored, longer scan times are disadvantageous.

All of the described methods require rather involved and costly modifications to a commercial CW laser FT-Raman spectrometer. In the case of the step-scan experiment, the conversion from a standard FT-Raman spectrometer currently costs >\$25 000. Also, none of these existing methods have been demonstrated to remove thermal backgrounds at temperatures of 300 °C or greater.

Herein we describe an inexpensive method for the real-time elimination of thermal backgrounds in FT-Raman spectra. The advantages of this method include an increase in signal/noise, no increase in single-spectrum acquisition time, the use of the preexisting FT-Raman software, the use of the a CW laser, and a total upgrade cost of ~\$3000. In addition, the described upgrade typically takes only a few hours to carry out and completely eliminates thermal backgrounds at temperatures in excess of 370 °C.

## EXPERIMENTAL SECTION

The instrumental setup for elimination of thermal backgrounds is shown in Figure 1. The output from the CW laser (1064 nm) is passed through an optical chopper (EG&G PAR Model 650) which is controlled via the internal oscillator of a dual-phase DSP lock-in amplifier (EG&G PAR Model 7260). A small fraction of the passed laser is sampled with a calibrated power meter which is part of a Nicolet 950 FT-Raman spectrometer. The chopped beam is focused into a fiber optic whose distal end is placed in the polymer sample within a temperature-controlled oven. Col-linear collection fibers collect both the thermal emission and the Raman scattered radiation and return it to the FT-Raman instrument. The voltage output from the detector (a BNC connector cable) is disconnected from the FT-Raman circuit board BNC connector and fed into the input channel of a dual-phase digital signal processor (DSP) lock-in amplifier. The X-output from the fast channel of the lock-in amplifier is connected back to the FT-Raman circuit board BNC connector. Spectral acquisition was performed using Nicolet Omnic software. Unless otherwise noted, a chop frequency of 2604.2 Hz was used and the time constant of the amplifier's digital filter output stage was set at 160  $\mu$ s.

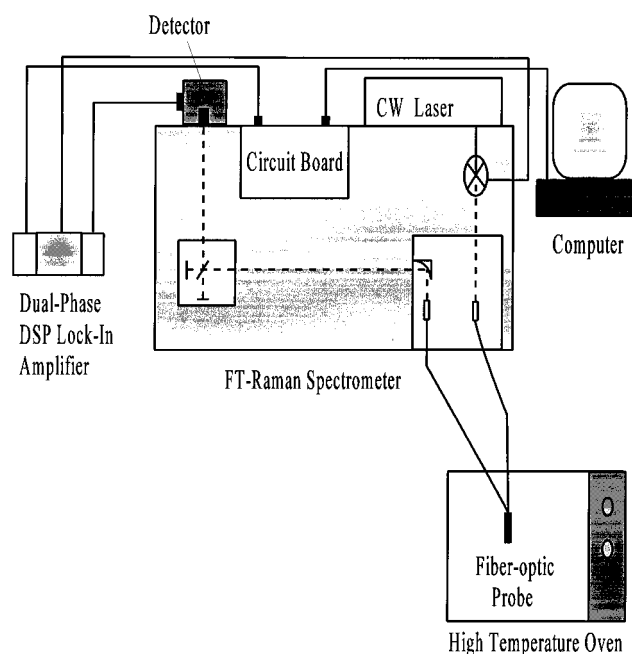


Figure 1. Modulated FT-Raman instrumental setup.

Amplification of the detector signal was set at 0 dB and 1 V full scale (i.e., no amplification).

For normal Raman experiments, the chopper wheel was adjusted so as not to interfere with the laser beam and the dual-phase DSP lock-in amplifier was disconnected from the instrument. In both types of experiments, identical incident laser powers were used (150 mW). The FT-Raman spectrometer was equipped with a liquid nitrogen-cooled germanium detector, a  $\text{CaF}_2$  beam splitter, and a  $\text{Nd:YVO}_4$  laser (1064 nm). All spectra were acquired at 8  $\text{cm}^{-1}$  resolution, using Happ–Genzel apodization, and a mirror velocity of 0.4747 cm/s, and consisted of a total of 100 scans (90 s total acquisition time). The temperature of the oven was continuously monitored using a thermocouple. The phenylethynyl-terminated polyimide was synthesized as previously described.<sup>11</sup>

## RESULTS

The fiber-optic FT-Raman spectra of a phenylethynyl-terminated polyimide (PETI) acquired at various temperatures are shown in Figure 2. When heated to temperatures in excess of 350 °C for an extended time, the ethynyl functional groups of this polymer react to form a network whose properties are suitable for many demanding aerospace applications. As shown, when the oven temperature exceeds 200 °C, a thermal background can be observed in the Stokes C–H stretching region of the spectrum ( $\sim 3100 \text{ cm}^{-1}$ ). By the time the temperature reaches 300 °C, the aromatic C–H stretch of the polymer can no longer be distinguished from the thermal background. At 350 °C, the thermal background extends out into the fingerprint portion of the Stokes region. In addition to the loss of vibrational information, the thermal background also results in an increase in spectral noise. Hence both qualitative and quantitative observations are difficult to make. At 375 °C, the thermal background resulted in a saturation of the A/D converter and no spectra could be collected.

In contrast, when the laser is modulated at 2604.2 Hz using the optical chopper, and the detector output is locked-in using

(8) Sakamoto, A.; Furukawa, Y.; Tasumi, M.; Masutani, K. *Appl. Spectrosc.* **1993**, *47*, 1457.

(9) Bennett, R. *Spectrochim. Acta* **1994**, *50*, 1813.

(10) Petty, C. Nicolet Instruments, PITTCON 1996, Atlanta, GA.

(11) Jensen, B. J.; Bryant, T. G.; Wilkinson, S. P. *Polym. Prepr. (Am. Chem. Soc., Div. Polym. Sci.)* **1994**, *35*, 559.

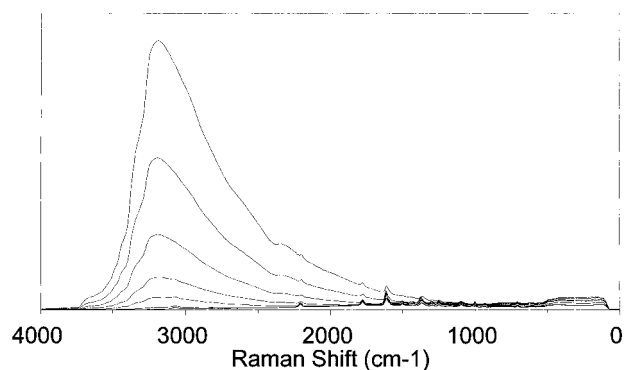


Figure 2. In situ fiber-optic FT-Raman spectra of PETI sample in an oven. The temperatures of the oven are (from top to bottom) 350, 325, 300, 275, 250, 100, and 30 °C. Incident laser power is 150 mW. A total of 100 scans were acquired for each spectrum.

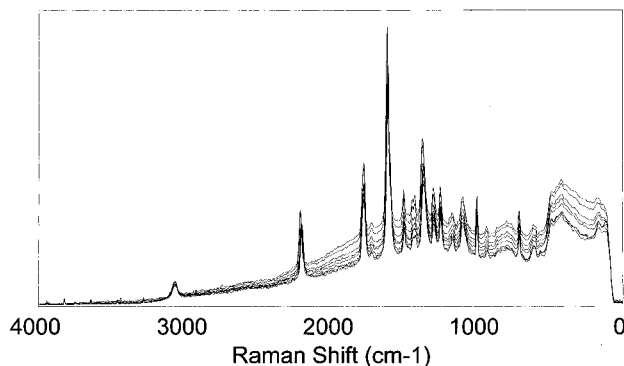


Figure 3. In situ fiber-optic modulated FT-Raman spectra of PETI sample in an oven. A modulation frequency of 2604.2 Hz was used. The temperatures of the oven are (from bottom to top) 350, 325, 300, 275, 250, 100, and 30 °C. Incident laser power is 150 mW. A total of 100 scans were acquired for each spectrum.

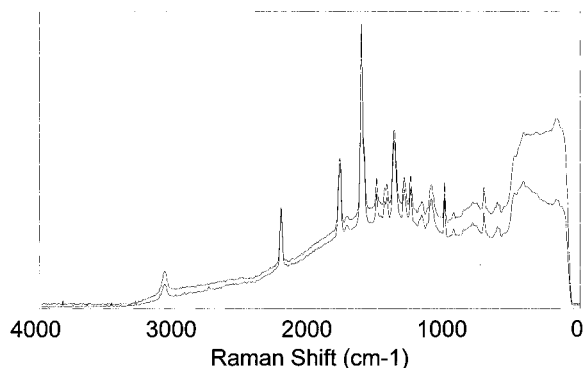


Figure 4. Overlay of fiber optic FT-Raman spectra of PETI at 30 °C both with and without modulation. The modulated spectrum has the lower fluorescence background and shows no distortion of Raman peaks. Both spectra are displayed on the same vertical axis.

the dual-phase DSP lock-in amplifier (modulated experiment), no thermal background is observed under identical conditions regardless of the temperature (Figure 3). A comparison of the resulting spectra from the two experiments at the lowest temperature (30 °C) and the highest temperature (350 °C) is given in Figures 4 and 5, respectively. At 375 °C, there was no saturation of the A/D converter for the modulated experiment, and a spectrum could be collected. As shown in Figure 4, the spectra are nearly identical. Relative peak intensities remain the same, as do bandwidth and resolution. The only noticeable difference is a slight decrease in the small fluorescent background for the modulated experiment. For the modulated experiment, small

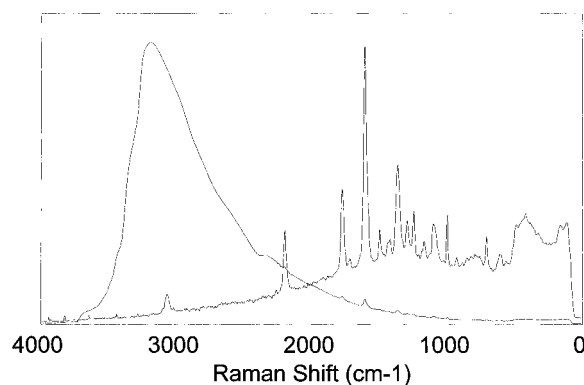


Figure 5. Overlay of fiber-optic FT-Raman spectra of PETI at 350 °C both with and without modulation. The modulated spectrum exhibits no thermal background. Both spectra are displayed with full vertical scales.

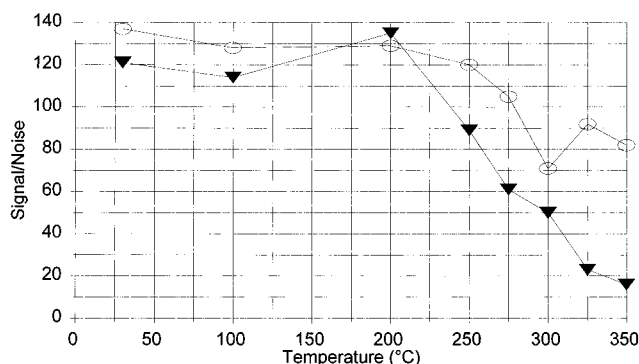


Figure 6. Signal/noise as a function of temperature for Raman spectra acquired using an FT-Raman spectrometer (triangles) and a modulated FT-Raman spectrometer (circles).

shifts to lower wavenumbers can be observed for both the ethynyl stretch ( $2150\text{ cm}^{-1}$ ) and the phenyl C–C stretch ( $1600\text{ cm}^{-1}$ ) as the temperature increases. This is a result of a decrease in the dihedral angle between the two phenyl rings that are bridged by the ethynyl group, giving rise to an increase in phenyl  $\pi$  donation into the ethynyl  $\pi^*$  orbital and causing a decrease in  $\pi$  bonding for both groups.

For both the modulated and the normal experiments, the signal/noise decreases as the temperature rises (Figure 6). However, it is worth noting that the signal/noise is higher for the modulated experiment at both low and high temperatures.

## DISCUSSION

In the modulated experiment, there are two modulations taking place. One involves the modulation of the laser ( $\nu_m$ ) and hence the modulation of the Raman modes. The second modulation ( $\nu_i$ ) is the result of the interferometer which results in all optical signals (including the thermal background) being modulated. Note that the  $\nu_i$  term is wavelength dependent. For the Raman signal, the mixing of these two modulation frequency terms results in detection of three terms:  $\nu_i$ ,  $\nu_i + \nu_m$ , and  $\nu_i - \nu_m$ , with an intensity ratio of 2:1:1, respectively.<sup>9</sup> Since the thermal background is only modulated by the interferometer, its frequencies are solely determined by the interferometer,  $\nu_i$ , and no mixing occurs. If the lock-in amplifier is referenced to the frequency of the laser modulation and the phases of the chop and the lock-in are synchronized (the purpose of the dual-phase option of the lock-in amplifier), then demodulation of the  $\nu_i + \nu_m$  and  $\nu_i - \nu_m$  terms yields an  $\nu_i$  term, and demodulation of the  $\nu_i$  term yields  $\nu_i - \nu_m$

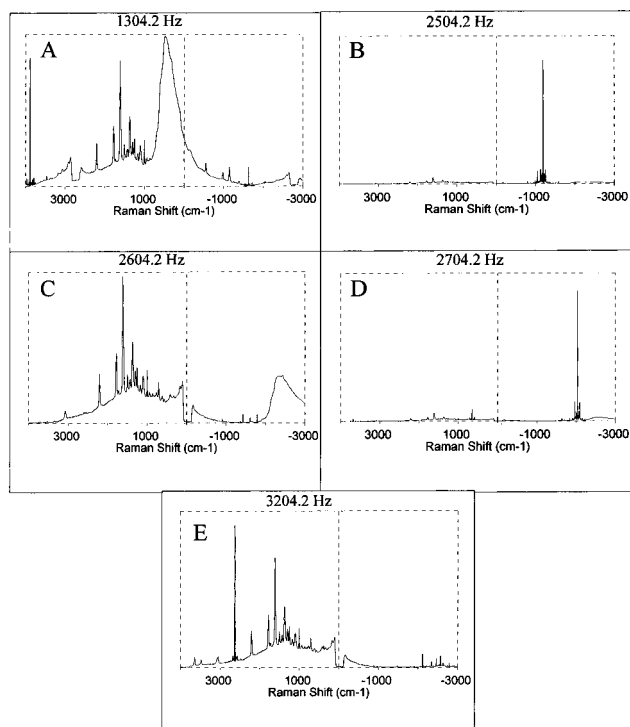


Figure 7. Modulated FT-Raman spectra of PETI acquired at 300 °C as a function of modulation frequency (A) 1304.2, (B) 2504.2, (C) 2604.2, (D) 2704.2, and (E) 3204.2 Hz. Spectra were acquired using a fiber-optic probe.

and  $\nu_i + \nu_m$  terms with intensity ratios of 2:1:1, respectively. After performing a Fourier transform on these terms, three spectra are obtained. The  $\nu_i$  term yields a normal Raman spectrum with the expected vibrational frequencies, while the other two terms correspond to identical spectra that are shifted to higher and lower frequencies by exactly the laser modulation frequency. The wavenumbers of these shifts are calculated by dividing the frequency by the interferometer mirror velocity (in cm/s). For the thermal background, demodulation via the lock-in amplifier results in two frequency terms:  $\nu_i + \nu_m$  and  $\nu_i - \nu_m$ . The final result after Fourier transformation is that there is no thermal component in the normal (unshifted) Raman spectrum.

In Figure 7A, the laser modulation frequency is 1304.4 Hz with an interferometer mirror velocity of 0.4747 cm/s. In addition to the normal Raman spectra, side spectra are expected at  $\pm 2747.8$  cm<sup>-1</sup>. Perhaps the easiest portion of the side spectra to follow is the notch filter (centered at a Stokes shift of 0), which is shifted by  $+\nu_m$  to give an apparent anti-Stokes shift of  $-2747.8$  cm<sup>-1</sup> and is also shifted by  $-\nu_m$  to give an apparent Stokes shift of  $2747.8$  cm<sup>-1</sup>. As expected, the normal unshifted Raman spectrum is also present. While the intense thermal background is present in the unmodulated spectrum (Figure 2) at approximately 3200 cm<sup>-1</sup>, the shifted background ( $\nu_i + \nu_m$ ) is expected at an apparent Stokes shift of 452 cm<sup>-1</sup>, as is observed. The  $\nu_i - \nu_m$  component of the thermal background is not observed since it lies outside of the spectral range (an apparent Stokes shift of  $+5948$  cm<sup>-1</sup>). Based on the spectrum in Figure 7A, it is clear that one consideration in using the modulated technique is to choose a modulation frequency which is sufficiently large to shift the side spectra out of the range of the normal Raman spectrum. This criterion is met when

$$\nu_m > (\hat{\nu}_S - \hat{\nu}_{AS}) \nu_{\text{mirror}} \quad (1)$$

where  $\nu_m$  is the laser modulation frequency in Hz,  $\hat{\nu}_{AS}$  is the maximum wavenumber at which anti-Stokes intensity is observed (expressed in terms of negative Raman shift),  $\hat{\nu}_S$  is the maximum wavenumber at which Stokes intensity is observed in an unmodulated experiment (expressed in terms of positive Raman shift), and  $\nu_{\text{mirror}}$  is the velocity of the mirror (in cm/s). For the PETI spectrum, in the absence of heat, this would correspond to the Stokes-shifted C-H stretch at 3050 cm<sup>-1</sup> and the decay of the fluorescence background to zero intensity at  $-1000$  cm<sup>-1</sup> to give a minimum modulation frequency of 1922.5 Hz if all spectral components are to be resolved. With the addition of a thermal background that extends to  $+3800$  cm<sup>-1</sup> before decaying to zero (Figure 2), the modulation frequency must be increased to 2278.6 Hz.

A second consideration in the modulated experiment is the choice of digital low-pass filters used following demodulation of the signals. It is essential that the low-pass filter pass all of the high optical frequencies if the Raman intensities are not to be perturbed. For this to occur, the time constant of the filter must be greater than the maximum spectral frequency which is not to be perturbed. For the PETI spectrum, the highest frequency component after lock-in demodulation corresponds to the fluorescent decay at  $-1000$  cm<sup>-1</sup> (absolute frequency of  $1000$  cm<sup>-1</sup> +  $9398.6$  cm<sup>-1</sup> =  $10398.5$  cm<sup>-1</sup> or 4936.2 Hz). Therefore, a time constant of 202  $\mu$ s or less would be required if the unshifted Raman spectrum is to appear as it would in the unmodulated experiment. If only the Stokes frequencies above 100 cm<sup>-1</sup> are important, then the time constant could be increased to 226  $\mu$ s. Unfortunately, for most DSP lock-in amplifiers, the filter time constant is not continuously tunable. For the present system, the available time constants in the  $\mu$ s range begin at 10  $\mu$ s and increase in a binary manner (e.g., 20, 40, 80, 160, 320, and 640  $\mu$ s). The optimum selection for such a system would therefore be 160  $\mu$ s. The general relation for the selection of the time constant is

$$(\hat{\nu}_L - \hat{\nu}_{AS}) \nu_{\text{mirror}} < 1/t \quad (2)$$

where  $\hat{\nu}_{AS}$  is the maximum anti-Stokes Raman wavenumber expressed in terms of negative shift,  $\hat{\nu}_L$  is the wavenumber of the laser,  $\nu_{\text{mirror}}$  is the velocity of the mirror (in cm/s), and  $t$  is the time constant of the digital output filter (in s).

For the current DSP lock-in amplifier, the fast time constants required for the modulated experiment are limited to the fast-output channel which has a filter slope of 6 dB/octave (an attenuation by 2 in amplitude for every 2-fold increase in frequency). This low slope value results in aliases not being fully attenuated. As shown in Figure 7, all of the spectra, except for the one acquired with a modulation frequency of 2604.2 Hz, exhibit aliases at frequencies corresponding to  $n\nu_m$ , where  $n$  is an integer. This alias results from the chopped Raman signal, which is not modulated by the interferometer due to the interferometer having a nonunity efficiency. The result is that at the input of the lock-in amplifier, a dc square wave of frequency  $\nu_m$  is introduced along with the interferometer frequency components discussed above. We have observed this square wave using an oscilloscope. When the square wave is demodulated at  $\nu_m$ , the result is a near-sinusoidal wave of frequency  $2\nu_m$  (observed with an oscilloscope

at the output channel). In the absence of output filtering, this alias results in an intense peak in the Raman spectrum regardless of the value of  $\nu_m$ . Since the alias frequencies lie in the same range as the optical frequencies, it is impossible to completely remove them with the output filter. However, if the A/D sampling frequency is a binary multiple of the modulation frequency (and hence the input square wave), the alias is completely eliminated with a time constant meeting the criteria of eq 3. The exact relation is

$$(\nu_{A/D})/(2^n) = \nu_m \quad (3)$$

where  $\nu_{A/D}$  is the sampling frequency of the A/D converter and  $n$  is an integer. In Figure 7,  $\nu_{A/D}$  was 166 669 Hz. A value of  $n = 6$  for the above expression yields a modulation frequency of 2604.2 Hz, which is where the alias is eliminated (Figure 7C). If a value of  $n = 7$  is used, a modulation frequency of 1302.1 Hz results. Experimentally this also results in elimination of the alias frequencies (Figure 7A still shows the remnants of the aliases since it was taken using a modulation frequency of 1304.4 Hz). When the A/D sampling frequency is shifted to 160 000 Hz, the alias frequencies are eliminated at 2500 Hz, as predicted. We have also collected spectra using a sampling frequency of 163 264 Hz which results in elimination of the alias frequencies when  $\nu_m = 2551$  Hz. We have also changed the mirror velocity to 0.316 cm/s, and eq 3 still remains valid for all three A/D sampling frequencies.

As described above, ideally the modulated experiment results in a 50% decrease in the Raman intensity (the other 50% being split into the side spectra) relative to an experiment where no modulation is used. This follows the treatment by Bennet and assumes a sinusoidal modulation. In fact, the modulation is a square wave, and sinusoidal demodulation results in further spectral intensity being lost to odd harmonics of the modulation frequency. The fact that the signal/noise for this technique is superior to that of the unmodulated technique even in the absence of heating suggests that lock-in amplification and digital filtering play a significant role in reducing the ultimate spectral noise. The signal/noise data presented in Figure 6 is based on the carbonyl stretching intensity (1770  $\text{cm}^{-1}$ ) for the intensity component and the rms noise of the adjacent spectral region (1900–2100  $\text{cm}^{-1}$ ). However, if the C–H stretching intensity (3050  $\text{cm}^{-1}$ ) is used, the signal/noise for the unmodulated experiment would drop to 0 at a temperature of 325 °C, since at this temperature the signal can no longer be observed. Thus, Figure 6 dramatically understates the improvement in signal/noise for the modulation technique when a thermal background is present.

Figure 8 displays three overlaid spectra of PETI taken at room temperature and at three different modulation frequencies: 0, 1480, and 2500 Hz. As  $\nu_m$  is increased, the slight fluorescent background decreases. This background cannot be due to glass Raman modes since these spectra were acquired within the sample compartment not using fiber optics. It is reasonable that this decrease is due to the temporal discrimination of the modulation technique. The Raman signal is instantaneous on the time scale of the instrument; however, the fluorescent state may have a lifetime which approaches that of  $\nu_m^{-1}$ . In this case, some of the fluorescent intensity would occur during the “off” portion of the modulation cycle and not be sampled by the lock-in amplifier. This suggests that for samples with long-lived emitting states which

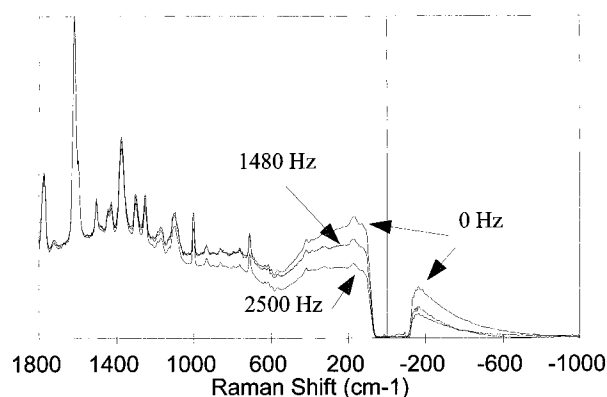


Figure 8. Overlay of intensity-normalized Raman spectra acquired using the modulated FT-Raman spectrometer at 2500, 1480, and 0 Hz. As the modulation frequency is increased, the fluorescent background decreases in intensity.

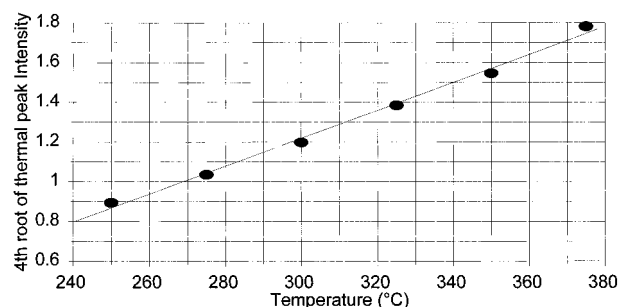


Figure 9. Calibration curve for sample temperature using the shifted and digitally filtered thermal peak intensity observed in the anti-Stokes region when modulating at 2604.2 Hz.

can be populated with 1064 nm radiation, the modulation technique may significantly reduce the fluorescent background. The decrease in signal/noise for the spectrum collected at 1480 Hz is due to the presence of large aliases (not shown) which result from the modulation frequency not adhering to the criterion of eq 3.

In Figure 2, the unmodulated technique results in a thermal peak whose intensity increases with temperature. The peak shape is a result of a drop off in the Ge detector sensitivity. When the modulation frequency is set to 2604.2 Hz, this thermal “peak” is shifted to the anti-Stokes region of the spectrum as shown in Figure 7C. In addition to being shifted, the peak is also attenuated. Part of this attenuation is due to the  $t = 160 \mu\text{s}$  output filter of the lock-in amplifier, while some of the intensity loss is due to the splitting of the total intensity between the  $\nu_1 + \nu_m$  and  $\nu_1 - \nu_m$  components. The net result at 300 °C is a thermal “peak” with an intensity similar to that of the Raman modes. For blackbody radiation, the total integrated intensity is related to the temperature by

$$T = kI^{1/4} \quad (4)$$

where  $k$  is a constant. As shown in Figure 9, a plot of this equation for the modulated experiment results in a linear relationship with a correlation coefficient of 0.991. This equation is only an approximation since the intensity of the blackbody radiation is also a function of the filter and only a portion of the blackbody radiation is collected. However, it does demonstrate that the resulting signal from the modulated experiment can be used to monitor the sample temperature. A more accurate calibration

could be obtained by fitting a line to the experimental data for a particular system/experiment. We have shown previously that the Raman anti-Stokes/Stokes intensity ratio for a thermoset vibrational mode whose intensity is independent of the sample cure can be used to monitor the sample temperature.<sup>2</sup> However, the correlation is not as good as the present method due to the weak intensity of the anti-Stokes modes and (in the case of PETI) the presence of the interfering fluorescence.

In comparing this technique to existing pulsed laser techniques for thermal background discrimination, one disadvantage is that the relatively long effective pulse width of the chopped laser ( $\text{fwhm} \approx \nu_m/2$ ) means that this technique will not be as effective in discriminating against laser induced heating when compared with techniques that use short pulse widths ( $<100$  ns). However, this also means that peak powers will not be any higher than in a conventional FT-Raman experiment and thus laser heating will not be as likely. We have also found that the Nicolet algorithms for removing scans with cosmic rays are not efficient when using this modulation technique; i.e., many good scans are eliminated.

The collection fiber optics used for this method are essential if maximum sample temperatures are to be reached. With the fiber optics, saturation of the detector occurs at approximately 380 °C. However, when a heated sample stage was placed within

the sample compartment of the instrument, temperatures in excess of 300 °C could not be reached.

## CONCLUSIONS

The described technique allows FT-Raman spectra to be collected at high temperatures using fast interferometer mirror velocities. For the investigated mirror velocities, modulation frequencies, and A/D sampling frequencies, no peak distortion is observed as a result of the modulation, and the signal/noise is superior to normal FT-Raman under identical experimental conditions. In addition, the shifted thermal signal can be used to accurately monitor the sample temperature in real-time.

## ACKNOWLEDGMENT

We gratefully acknowledge the National Aeronautics and Space Administration (Grant NGT152124) and the National Science Foundation (Grant DMR9414000) for their financial support of this work.

Received for review February 18, 1997. Accepted April 1, 1997.<sup>⊗</sup>

AC970193H

---

<sup>⊗</sup> Abstract published in *Advance ACS Abstracts*, May 1, 1997.